JOURNAL OF MAGNETIC RESONANCE **134,** 72–75 (1998)
ARTICLE NO. MN981529

Efficient Simulation of ESEEM Spectra Using Gamma

Johan J. Shane, Lorenz P. Liesum, and Arthur Schweiger

Laboratorium für Physikalische Chemie, Eidgenössische Technische Hochschule, CH-8092, Zürich, Switzerland

Received April 10, 1998

Using the Gamma class library for C++ it is possible to write very efficient time-domain simulation programs for echo-detected pulse EPR experiments, such as three-pulse ESEEM and HYSCORE. By grouping sections of time-invariant propagators, the initial density operator and the detection operator can be redefined, and the simulation transforms to that of a free induction decay which can be evaluated very efficiently using elements from Gamma. Compared to a straightforward implementation, reductions in computing time of up to a factor of 673 have been found.

INTRODUCTION

The most straightforward way to simulate the time evolution of a pulse magnetic resonance experiment is to let a density operator evolve from its initial state through the different time intervals of the experiment. The development of such a simulation program is greatly simplified by using the computer package Gamma (*1*).

Gamma is widely used for the simulation of NMR experiments (*2–6*), but there have been only a few publications where Gamma is applied to simulate pulse EPR spectra (*7–10*). One of the reasons for this might be the presumed inefficiency of time-domain simulations of electron spin-echo experiments. It is usually more efficient to calculate the frequencies and transition probabilities, and then to construct the spectrum in the frequency domain. Indeed there are several programs in use that are based on this approach (*11–13*).

In this communication we will demonstrate that by using the optimized features of Gamma, time-domain simulations of echo-detected pulse EPR experiments can actually be performed very efficiently if care is taken in writing the simulation programs. Reductions in computing time of between two and three orders of magnitude have been found, depending on the complexity of the experiment and on the number of data points in the simulation.

THEORY

Using the density operator formalism, the echo intensity of the three-pulse ESEEM experiment, $\pi/2{-}\tau{-}\pi/2{-}T{-}\pi/2{-}\tau{-}echo$, shown in Fig. 1a is given by (*14*)

$$E(\tau, T) = \mathrm{Tr}\{R_\tau R_P R_T R_P R_\tau R_P \sigma_0 R_P^{-1} R_\tau^{-1} R_P^{-1} R_T^{-1} R_P^{-1} R_\tau^{-1}\, S_x\}, \quad [1]$$

where R_τ and R_T are the propagators for the free evolution during the times τ and T, R_P is the propagator describing the non-selective, ideal $\pi/2$ pulses along the rotating frame y-axis, and σ_0 is the initial density operator. The echo signal is observed along the x-axis. Matrix representations for all the operators can easily be generated, so that a numerical calculation of $E(\tau, T)$ is straightforward, but time-consuming. The simulation of a three-pulse ESEEM experiment involves the evaluation of $E(\tau, T)$ for a large number of T values. Table 1 shows the relevant section of a program using the Gamma software package, with a suitably defined Hamiltonian (`H`) of the spin system (`spin`).

No analytical expression for the modulation intensity is needed, and non-ideal pulses can be included very easily by calculating an appropriate Hamiltonian and replacing the `Iypuls` function call. The disadvantage of this approach is obviously the repetition of the calculation for all values of T. The computation is even more time-consuming when phase cycling needs to be included in the simulation, which is almost always the case. A separate calculation has then to be performed for every cycle.

The inefficient simulation procedure sketched above can however be simplified considerably. Several parts of Eq. [1] are the same for each value of T. It is therefore prudent to pre-calculate these. Since the trace is invariant under a cyclic permutation of operators, Eq. [1] can be re-ordered to

$$\begin{aligned} E(\tau, T) &= \mathrm{Tr}\{(R_P R_\tau R_P \sigma_0 R_P^{-1} R_\tau^{-1} R_P^{-1})\, R_T^{-1} (R_P^{-1} R_\tau^{-1} S_x R_\tau R_P)\, R_T\} \\ &= \mathrm{Tr}\{\sigma_1 R_T^{-1} D\, R_T\}, \end{aligned} \quad [2]$$

where

$$\sigma_1 = R_P R_\tau R_P \sigma_0 R_P^{-1} R_\tau^{-1} R_P^{-1} \quad [3]$$

and

$$D = R_P^{-1} R_\tau^{-1} S_x R_\tau R_P. \quad [4]$$

1090-7807/98 $25.00

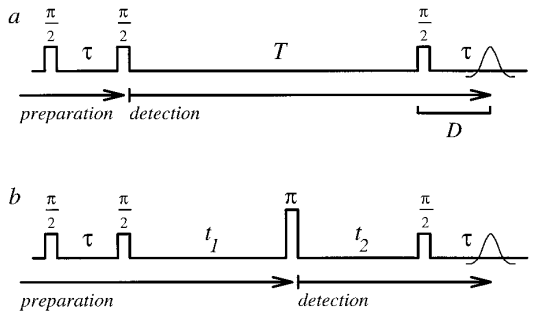

FIG. 1. (a) One-dimensional three-pulse ESEEM sequence. D indicates the section of the pulse sequence which is taken into the effective detection operator in the new approach. (b) Two-dimensional HYSCORE sequence. The evolution during t_1 is taken into the time-independent preparation section.

Equation [3] describes the preparation sequence, $\pi/2$–τ–$\pi/2$, which is the same for all time-intervals T. D, defined by Eq. [4], replaces S_x as the detection operator, and defines the segment of the sequence starting from the third $\pi/2$ pulse. This is in line with the subdivision of a pulse sequence into a preparation, a mixing, and a detection period (*15*). The preparation and detection periods of the three-pulse ESEEM experiment as defined by Eqs. [3] and [4] are indicated in Fig. 1a.

Equation [2] suggests that the ESEEM signal can be viewed as a free induction decay, where the detection operator is D, rather than S_x. Gamma has very efficient functions to calculate such free induction decays. Using the function `FID`, we can re-write the program code as is shown in Table 2. The loop over T in the program has been replaced by a call to the `FID` function, which internally performs the loop in a highly optimized fashion. The use of this function reduces the computation time considerably.

PHASE CYCLING

Phase cycling is used to remove unwanted echoes and free induction decays. This is done by adding the signals from experiments with different phases of the microwave pulses in such a way that only the stimulated echo remains. This is equivalent to selecting one specific coherence transfer pathway from all possible pathways (*16*).

One way to select a specific pathway is to remove all undesired elements from the density matrix at specific points in time during the experiment. This very efficient procedure cannot, however, be incorporated in the formalism described above, because it cannot be expressed as an operator in Hilbert space. The only alternative is to explicitly perform the phase cycling and to add the signals of the separate experiments. This summation can be performed in the calculation of the preparation density operator σ_1 and of the detection operator D.

If the cycled pulse occurs before the free evolution time T, it only affects the calculation of σ_1. The summation of an n-step phase cycle yields

$$E(\tau, T) = \sum_i^n \mathrm{Tr}\{R_T \sigma_{1i} R_T^{-1} D\} = \mathrm{Tr}\{R_T \sigma_1' R_T^{-1} D\}, \qquad [5]$$

where $\sigma_1' = \Sigma_i^n \sigma_{1i}$ is a new density operator which incorporates the coherence transfer pathway selection up to the start of the T evolution. Similarly, phase cycling after the free evolution leads to different detection operators D, which can be summed to a total detection operator D', incorporating the coherence pathway selection after time T.

OTHER PULSE EPR SEQUENCES

The formalism described here can easily be expanded to other pulse EPR experiments. For each pulse scheme, an appropriate preparation and detection sequence has to be defined.

In two-dimensional experiments, the echo is a function of two time variables. The new approach can be expanded to encompass multi-dimensional experiments by treating them as a series of one-dimensional experiments. The calculation of the FID in Eq. [2] is repeated for every slice of the two-dimensional experiment. The time variables that remain constant in that slice are taken into the invariant preparation or detection segments, as indicated in Fig. 1b. For example, the HYSCORE (*16, 17*) and DEFENCE (*18*) experiments can be treated in the same way. The simulation for the DEFENCE experiment rep-

TABLE 1
C++ Code Fragment for a Simulation Program Written Using a Straightforward Approach

```
for (T = 0, i = 0; i < size; T += dT, ++i) {
  sigma = Iz (spin, 0);
  sigma = Ypuls (spin, sigma, 90, 0);
  evolve_ip (sigma, H, tau);
  sigma = Ypuls (spin, sigma, 90, 0);
  evolve_ip (sigma, H, T);
  sigma = Ypuls (spin, sigma, 90, 0);
  evolve_ip (sigma, H, tau);
  echo [i] = trace (sigma * Ix (spin, 0));
}
```

TABLE 2
C++ Code Fragment for a Simulation Written Using the New Approach

```
D = Ix (spin, 0);
evolve_ip (D, H, -tau);
D = Ypuls (spin, D, -90, 0);
sigma = Iz (spin, 0);
sigma = Ypuls (spin, sigma, 90, 0);
evolve_ip (sigma, H, tau);
sigma = Ypuls (spin, sigma, 90, 0);
FID (sigma, D, H, or T, size, echo);
```

resents one slice of the simulation of the HYSCORE experiment.

For pulse schemes using probe-pulse detection (*19, 20*), the full time trace is measured in a single experiment. In this case the new simulation approach closely matches the experiment. The preparation sequence encompasses the whole pulse sequence, and the detection operator remains unchanged. Similarly, in hole-burning experiments (*21*) the signal already represents a free induction decay. No reduction in computing time is expected for these experiments.

The method described in this Communication is only applicable if the calculation can be re-ordered according to Eq. [2]. There are some types of experiments where this is not possible, although the grouping of the pulse sequence in invariant segments may still simplify the calculation. In most pulse ENDOR experiments, such as Davies-ENDOR and Mims-ENDOR (*22, 23*), all time intervals remain constant. For two-pulse ESEEM and related approaches, such as the two-dimensional combination peak experiment (*10*), the applicability of the formalism is also limited. In the case where two time intervals are changed simultaneously, it is not possible to write the echo signal in the form of Eq. [2]. The propagator $R_\tau R_P R_\tau$ cannot in general be written as $R'_\tau = e^{-i\mathcal{F}\tau}$ for some operator $\mathcal{F}$, and it is not possible to use the efficient FID calculation of Gamma.

RESULTS

Two sets of comparative simulations were performed on a Sparc Ultra 1 workstation with 128 MB RAM, using the GNU C++ compiler version 2.5.8.

Computation times for one-dimensional three-pulse ESEEM and two-dimensional HYSCORE simulations using the straightforward approach and the new approach are listed in Tables 3 and 4, respectively. The simulations are for a single orientation of a system consisting of one electron spin coupled to one proton (ESEEM simulations) or two protons (HYSCORE simulations), with axially symmetric anisotropic hyperfine interactions. The results show that the reduction in computation time depends on the complexity of the experiment and on the number of data points in the simulation. In our examples, it amounts to up to a factor 673.

TABLE 3

Comparison of Computation Times for the One-Dimensional Three-Pulse ESEEM Experiments, for a Single Orientation of a One-Electron, One-Proton System

Size of time trace	Straightforward approach	New approach	Reduction in computing time
128	165 ms	1.67 ms	99
256	332 ms	1.95 ms	171
512	672 ms	2.38 ms	282
1024	1.33 s	3.41 ms	390

TABLE 4

Comparison of Computation Times for the Two-Dimensional HYSCORE Experiment, for a Single Orientation of a One-Electron, Two-Proton System

Size of time domain	Straightforward approach	New approach	Reduction in computing time
128 × 128	87.2 s	0.395 s	221
256 × 256	346 s	0.971 s	357
512 × 512	1386 s	2.66 s	521
1024 × 1024	5546 s	8.24 s	673

For simulations of short time traces, the computation time is dominated by the calculation of the initial density operator σ_1 and of the detection operator D. For simulations of longer time traces, the computation time of the FID, which increases linearly with the size of the time trace, dominates. Hence, complicated experiments with large data sets benefit more from the new approach.

CONCLUSIONS

Simulations of echo-modulation experiments for which no analytical expression for the modulation amplitude exists can in general be performed very efficiently using the new computation approach presented here. The method also allows the calculation of powder spectra with little computing time.

In cases where analytical expressions do exist, it is generally more efficient to directly simulate the frequency-domain spectra. Such expressions exist for the two-pulse ESEEM, three-pulse ESEEM, and HYSCORE experiments, with ideal, nonselective pulses and nuclei with spin $I = 1/2$.

Frequency-domain simulations can also be based on generalized expressions of the modulation amplitude for spin systems with arbitrary nuclear spins (*14, 24*), which give the modulation amplitude in terms of the transition probabilities for ideal pulses.

For comparison, the simulation of a 256-by-256 point frequency-domain HYSCORE spectrum using a frequency-domain simulation with 225 orientations for the same system as described above, is reported (*13*) to take 2.47 seconds on a Digital Alpha workstation (DEC 3000).

In many cases, however, frequency domain simulations are not feasible, for instance because there are no analytical expressions available for the experiment, the pulses are not ideal, the electron spin quantum number S is larger than 1/2, or the high-field approximation is not valid. In these cases, the new approach presented here provides a very promising alternative for the simulation of echo-detected pulse EPR spectra.

REFERENCES

1. S. A. Smith, T. O. Levante, B. H. Meier, and R. R. Ernst, *J. Magn. Reson. A* **106,** 75 (1994).

2. M. Baldus, T. O. Levante, and B. H. Meier, *Z. Naturforsch.* **49,** 80 (1994).
3. M. R. Conte, C. J. Bauer, and A. N. Lane, *J. Biomol. NMR* **7,** 190 (1996).
4. M. Ernst, S. Bush, A. C. Kolbert, and A. Pines, *J. Chem. Phys.* **105,** 3387 (1996).
5. J. Huth, R. Q. Fu, and G. Bodenhausen, *J. Magn. Reson. A* **123,** 87 (1996).
6. R. Graf, D. E. Demco, J. Gottwald, S. Hafner, and H. W. Spiess, *J. Chem. Phys.* **106,** 885 (1997).
7. M. Willer and A. Schweiger, *Chem. Phys. Lett.* **230,** 67 (1994).
8. G. Jeschke and A. Schweiger, *Mol. Phys.* **88,** 355 (1996).
9. A. Ponti, *J. Magn. Reson.* **127,** 87 (1997).
10. S. Van Doorslaer and A. Schweiger, *Chem. Phys. Lett.* **281,** 297 (1997).
11. C. P. Keijzers, E. J. Reijerse, P. Stam, M. F. Dumont, and M. C. M. Gribnau, *J. Chem. Soc. Faraday Trans.* **83,** 3493 (1987).
12. M. J. Mombourquette and J. A. Weil, *J. Magn. Reson.* **99,** 37 (1992).
13. D. Goldfarb, private communication.
14. W. B. Mims, *Phys. Rev. B* **5,** 2409 (1972).
15. A. Schweiger, *J. Chem. Soc. Faraday Trans.* **91,** 177 (1995).
16. C. Gemperle, G. Aebli, A. Schweiger, and R. R. Ernst, *J. Magn. Reson.* **88,** 241 (1990).
17. P. Höfer, A. Grupp, H. Nebenfür, and M. Mehring, *J. Chem. Phys.* **132,** 279 (1986).
18. A. Ponti and A. Schweiger, *J. Chem. Phys.* **102,** 5207 (1995).
19. M. K. Bowman, *Isr. J. Chem.* **32,** 339 (1992).
20. E. Hoffmann and A. Schweiger, *Chem. Phys. Lett.* **220,** 467 (1994).
21. T. Wacker, G. A. Sierra, and A. Schweiger, *Isr. J. Chem.* **32,** 305 (1992).
22. E. R. Davies, *Phys. Lett. A* **47,** 1 (1974).
23. W. B. Mims, *Proc. R. Soc. London A* **283,** 452 (1965).
24. J. J. Shane, P. Höfer, E. J. Reijerse, and E. de Boer, *J. Magn. Reson.* **99,** 596 (1992).